

Identification of an *N*-Methyl-D-aspartate Receptor in Isolated Nervous System Mitochondria*

Received for publication, November 8, 2011, and in revised form, August 22, 2012. Published, JBC Papers in Press, August 23, 2012, DOI 10.1074/jbc.M111.322032

Amit S. Korde[‡] and William F. Maragos^{‡§1}

From the [‡]Neurology Service, Hunter Holmes McGuire Veterans Hospital, Richmond, Virginia 23249 and the [§]Department of Neurology, Virginia Commonwealth University, Richmond, Virginia 23298

Background: The accumulation of calcium by mitochondria regulates cell survival.

Results: Purified mitochondria exhibit increased calcium uptake in the presence of NMDA receptor agonists.

Conclusion: Functional NMDA-like receptors may be present on mitochondria.

Significance: Learning how NMDA facilitates mitochondrial calcium uptake provides a new dimension to the understanding of cellular homeostasis and response to noxious stimuli.

NMDA ionotropic glutamate receptors gate the cytoplasmic influx of calcium, which may, depending on the intensity of the stimulus, subserve either normal synaptic communication or cell death. We demonstrate that when isolated mitochondria are exposed to calcium and NMDA agonists, there is a significant increase in mitochondrial calcium levels. The agonist/antagonist response studies on purified mitochondria suggest the presence of a receptor on mitochondria with features similar to plasma membrane NMDA receptors. Immunogold electron microscopy of hippocampal tissue sections revealed extensive localization of NR2a subunit immunoreactivity on mitochondria. Transient transfection of neuronal GT1-7 cells with an NR1-NR2a NMDA receptor subunit cassette specifically targeting mitochondria resulted in a significant increase in mitochondrial calcium and neuroprotection against glutamate-induced cell death. Mitochondria prepared from GT1-7 cells in which the NR1 subunit of NMDA receptors was silenced demonstrated a decrease in calcium uptake. Our findings are the first to demonstrate that mitochondria express a calcium transport protein that shares characteristics with the NMDA receptor and may play a neuroprotective role.

The plasma membrane NMDA ionotropic glutamate receptor subtype has long been recognized to be involved in synaptic communication and to underlie normal brain functions such as learning and memory (1). Located ubiquitously on neurons throughout the brain, NMDA receptors have also been implicated in neurodegenerative conditions such as stroke, Huntington disease, and HIV dementia (2, 3). Pathological activation of NMDA receptors, either by direct or indirect mechanisms, results in excessive Ca^{2+} influx into the cytoplasm, which can lead to cell death (4). The mechanism of neurodegeneration is complex, and activation of a host of enzymes, including cal-

cinurin, nitric-oxide synthase, calpain, and MAPK, as well as inhibition of the phosphatidylinositol 3-kinase/Akt pathway may be involved (for review, see Ref. 5).

Mitochondria serve to buffer cytoplasmic Ca^{2+} resulting from activation of plasma membrane NMDA receptors (6–8). In the nervous system, mitochondrial Ca^{2+} uptake is mediated primarily by a Ca^{2+} uniporter, and the driving force for its action is the mitochondrial membrane potential (9). A rapid access mode (RAM)² of Ca^{2+} uptake into mitochondria has also been described (10). The precise role that each of these pathways plays in buffering cytoplasmic Ca^{2+} following plasma membrane NMDA receptor stimulation is not well understood. Interestingly, this pool of Ca^{2+} appears to have privileged access to mitochondria (11), although how this occurs is not known.

Considerable evidence has amassed that in addition to its role as a nervous system neurotransmitter, glutamate may also activate receptors on a variety of non-neuronal cells, including osteoclasts (12), platelets (13), and keratinocytes (14, 15), as well as several carcinomas (16, 17). In several of these cell types, the expression of NMDA receptors has been reported (18–21). In pancreatic islet cells, intracellular glutamate may be coupled to insulin secretion (22). Although these latter findings have been debated (23), they raise the intriguing possibility that glutamate could serve as an important intracellular signaling factor. On the basis of these observations and the link between NMDA-stimulated mitochondrial uptake of Ca^{2+} , we sought to determine whether purified mitochondria are sensitive to the direct actions of NMDA receptor agonists.

EXPERIMENTAL PROCEDURES

Animals—Male Sprague-Dawley rats 12–16 weeks of age were used for these studies. All animal use procedures were in accordance with the National Institutes of Health Guide for the Care and Use of Laboratory Animals and were approved by the University of Kentucky and Hunter Holmes McGuire Veterans Hospital Institutional Animal Care and Use Committees.

* This work was supported, in whole or in part, by National Institutes of Health Grants NS01941 and NS42111 (to W. F. M.) and McGuire Veterans Administration Medical Center and McGuire Research Institute.

¹ To whom correspondence should be addressed: Neurology Service, Hunter Holmes McGuire Veterans Hospital, Rm. 2B-175, 1201 Broad Rock Blvd., Richmond, Virginia 23294. Tel.: 804-675-5000 (ext. 3743); Fax: 804-675-5939; E-mail: william.maragos@va.gov.

² The abbreviations used are: RAM, rapid access mode; OMM, outer mitochondrial membrane(s); IMM, inner membrane-containing mitoplast(s); FU, fluorescence units.

Mitochondrial Preparation—A recently described method (24) was used with the modification that samples of cerebral cortex were placed into a large manual glass homogenizer containing 5 ml of ice-cold isolation buffer (20 mM HEPES, 215 mM mannitol, 75 mM sucrose, 0.1% BSA, and 1 mM EGTA, pH 7.2) that contained several inhibitors to prevent the influx and efflux of Ca^{2+} during the preparation of mitochondria (25, 26). This “locking buffer” contained 16 μM ruthenium red to block the mitochondrial inward transport of Ca^{2+} via the uniporter and RAM and extrusion via the sodium-independent antiporter, 15 μM cyclosporin A to prevent movement of Ca^{2+} via the permeability transition, and 10 μM CGP-37157 to inhibit outward flux of Ca^{2+} via the sodium-dependent antiporter. Neither Na^+ , which is required for activation of the sodium-independent antiporter, nor EGTA/EDTA was included in this buffer.

Mitochondrial Calcium Assays—For single time point mitochondrial calcium concentration ($[\text{Ca}^{2+}]_m$) determination, 50 μg of mitochondria were incubated in assay buffer A (20 mM HEPES, 215 mM mannitol, 75 mM sucrose, 2.5 mM KH_2PO_4 , and 0.1% fatty acid-free BSA, pH 7.2) containing 5 μM CaCl_2 and various combinations of NMDA receptor agonists and antagonists in a final volume of 100 μl . Following a 30-min incubation at room temperature, the samples were centrifuged at $10,000 \times g$ for 10 min at room temperature. The mitochondrial pellet was taken up in 100 μl of assay buffer A and added to a 96-well culture dish to which 5 μM Calcium Green-5N (Invitrogen) was added. Fluorescence (base-line) measurements were made in the intact mitochondria and then repeated 15 min following the addition of 1% Triton X-100 to lyse mitochondria and liberate matrix Ca^{2+} . Fluorescence was measured using an excitation wavelength of 485 nm and an emission wavelength of 532 nm. In a single experiment, $[\text{Ca}^{2+}]_m$ was measured directly using the fluorescent probe Rhod-2 (Invitrogen). All steps performed were identical to those describe above with the exceptions that mitochondria were preloaded with 10 μM Rhod-2 prior to a 30-min incubation with NMDA and/or calcium, and the mitochondria then washed three times. Fluorescence was measured using an excitation wavelength of 552 nm and an emission wavelength of 581 nm. Protein concentrations were determined using the Bradford protein assay (Pierce). All experiments were replicated three to six times.

The effect of NMDA on $[\text{Ca}^{2+}]_m$ was also measured in real-time. Mitochondria were prepared as described above with the exception that no calcium transporter-blocking agents were included in either the isolation or assay buffer. A 250- μg sample of mitochondrial protein was added to a cuvette that contained 2 ml of assay buffer B (20 mM Tris-HCl, 150 mM sucrose, 50 mM KCl, 2 mM KH_2PO_4 , and 5 mM succinate, pH 7.2) and 0.5 μM Calcium Green-5N. Bolus additions of calcium (5 μM) were injected at regular intervals in the absence or presence of 10 μM NMDA. Fluorescence was measured in a PerkinElmer LS 55 spectrofluorometer with excitation and emission wavelengths of 500 and 535 nm, respectively. Samples were continuously stirred and maintained at 37 °C during the recordings.

Western Blot Analysis—Samples of cytosol, synaptic membrane fragments, or mitochondria were probed with antibodies using standard methodology. The following primary antibodies were used at a dilution of 1:2000: β -actin (Sigma); cytochrome

oxidase subunit IV, NR2a, and NR1 (Molecular Probes, Eugene, OR); and LAMP1 and calnexin (Sigma). Antibodies against synaptophysin (Abcam, Cambridge, MA) and β -subunit Na^+, K^+ -ATPase (BD Transduction Laboratories) were used at a dilution of 1:20,000. ECL detection reagent was used to develop gels, which were imaged either directly on film or using a Fuji LAS4000 image analyzer. In some instances, films were scanned, and the optical densities were measured.

Electron Microscopy—Immunogold labeling was performed on rat brain tissue (hippocampal CA1 subregion) and mitochondrial pellets that were fixed with 4% paraformaldehyde and 0.25% glutaraldehyde in Sorenson's buffer and infiltrated with LR White resin using standard procedures. For routine electron microscopy, mitochondrial pellets were simply fixed and infiltrated. Sections were cut on a Leitz ultramicrotome and collected on nickel grids. Immunolabeling was performed using a 1:50 to 1:25 dilution of a monoclonal antibody against rat NR2a (Invitrogen) and 12–15-nm colloidal gold conjugated to a goat anti-rabbit secondary antibody (1:25; Jackson Immuno-Research Laboratories, West Grove, PA). Sections were counterstained with uranyl acetate and lead citrate. The grids were examined and photographed on a Hitachi H-7100 transmission electron microscope.

Mitochondrial Membrane Solubilization—Inner and outer mitochondrial membranes were separated using digitonin fractionation. Briefly, 1 mg of purified mitochondria was added to 1% digitonin on ice for 10 min, after which the sample was diluted with an equal volume of isolation buffer, followed by centrifugation at $12,000 \times g$ for 10 min at 4 °C. The resultant supernatant contained the outer mitochondrial membrane (OMM), and the pellet contained inner membrane-containing mitoplasts (IMM). The supernatant was centrifuged at $145,000 \times g$ for 1 h at 4 °C, and the resultant pellet was resuspended in 1 ml of 100 mM Na_2CO_3 for 5 min on ice and then centrifuged at $145,000 \times g$ at 4 °C to obtain highly purified OMM. The mitoplast fraction was resuspended in isolation buffer on ice, sonicated for 1 min, and centrifuged for $12,000 \times g$ for 10 min at 4 °C. The resulting supernatant was centrifuged at $145,000 \times g$ for 1 h at 4 °C. The pellet containing the IMM was resuspended in 1 ml of 100 mM Na_2CO_3 for 5 min on ice and centrifuged at $145,000 \times g$ at 4 °C to obtain pure IMM. For Western blotting, the OMM and IMM were probed with antibodies against the voltage-dependent anion channel and adenine nucleotide translocator, respectively (Abcam).

Bcl-2-NR1-NR2a Fusion Protein Construct—The *GRINA* and *GRIN2A* genes were subcloned into a single bicistronic vector (pCMV-BICEPTM-4, Sigma) in tandem to create a fusion protein of NR1-NR2a. The vector consists of multiple cloning sites: for *GRINA*, the site was EcoRI/XbaI, and for *GRIN2A*, the site was HindIII/EcoRI. To target the mitochondria, the Bcl-2 mitochondrial leader sequence was added. The leader amino acid sequence was MLSLRQSIRFFKPATRTL. The N terminus of the sequence was modified by adding the unique restriction site MseI, and the C terminus was modified by adding BamHI, which allowed insertion of the leader sequence immediately downstream of the promoter and upstream of the NR1-NR2a sequence. Also, the reading frames of the leader and both genes (*GRINA-GRIN2A*) were continuous. The construct was ampli-

NMDA Enhances Calcium Uptake in Isolated Mitochondria

fied using the following primers: forward, 5'-CGGGAGAAT-GTCTGGACCTA-3'; and reverse, 5'-TTCTGTGACCAGTC-CTGCTG-3'. A mutant construct was created by introducing a single point mutation (T648A) in the glutamate-binding region of *GRINA* using site-directed mutagenesis (Agilent Technologies, Santa Clara, CA).

Cell Culture and NMDA Receptor Overexpression—GT1-7 cells, which are immortalized hypothalamic neurons, were cultured in modified DMEM containing 4500 mg/liter glucose, 110 mg/liter pyruvate, and 548 mg/liter L-glutamine (Mediatech, Herndon VA), 10% fetal calf serum (Invitrogen), and 1% penicillin/streptomycin (Invitrogen). Cultures were maintained at 37 °C in an incubator kept at 5% CO₂. Cultures were passed by treating with 1× trypsin (Sigma) diluted in 1× phosphate-buffered saline for 1–2 min at room temperature. Culture flasks were passed every week, and for all studies, cells were used between passages 5 and 10.

Using 6-well plates that were seeded at a density of 100,000 cells/well, transient transfection was performed with the commercially available transfection agent Lipofectamine 2000 (Invitrogen). Briefly, transfections were carried out in wells containing 2 ml of medium and cells that were ~80% confluent. One μg of DNA and 7 μl of Lipofectamine 2000 in 3 ml of Opti-MEM medium (Invitrogen) were added to each well. After a 6-h incubation, the transfection mixture was replaced with culture medium. In initial experiments using a GFP-tagged construct, expression efficiency was calculated to be ~85%. In these experiments, expression was confirmed at 48–72 h by obtaining preparing mitochondria from the cells and performing Western blot analysis for NR1 and NR2a.

Toxicity Assays—The effects of glutamate agonists were examined at 48–72 h following transfection. Cells were exposed to 25 μM L-glutamate for 15 min, after which the medium was replaced with fresh medium. Twenty-four h later, live and dead cells were quantified using a LIVE/DEAD viability/cytotoxicity kit (Invitrogen) following the protocol provided by the manufacturer. Live and dead cells were visualized with a Zeiss Axiovert fluorescence microscope. A manual counter was used to record the number of live and dead cells. At least 150–200 cells/well were counted (at 12, 3, 6, and 9 o'clock and the center of each well), and each sample was run in triplicate. For calcium assays, cells were exposed to 25 μM L-glutamate for 15 min, after which mitochondria were prepared from 10⁶ cells in locking buffer, and calcium was quantified as previously described. Experiments were repeated three times.

ATP Assay—Non-transfected, transfected, and mutant-transfected GT1-7 cells were exposed to 25 μM L-glutamate for 30 min, after which reaction buffer was added to the wells, and ATP concentrations were measured using a commercially available ATP kit (Molecular Probes). A standard curve was generated using standards provided by the manufacturer. Samples were measured in a Molecular Devices SpectraMax Plus luminometer at 560 nm, and ATP levels were extrapolated from the standard curve. Each experiment was repeated three times.

Gene Silencing—Human NMDA NR1 (transcript variant 2) siRNA with sequence 5'-ACA ATG AGC GTG CGC AGT A-3' was obtained commercially (Integrated DNA Technologies, Coralville, IA). One μg of siRNA and 6 μl of Lipofectamine

2000 were mixed in 2 ml of Opti-MEM medium for 15 min at room temperature and then applied to 90% confluent GT1-7 cells. Cells were cultured in a 5% CO₂ incubator at 37 °C for 72 h. Cells in the control groups were either non-transfected or transfected with the scrambled siRNA (5'-GCUUA-CUGCGUAUAGGUCACA-3'). The efficiency of NMDA NR1 gene silencing was determined by Western blot analysis. Cell lysates (10 μg of protein) were loaded onto a 4–12% SDS resolving gel and then transferred to a nitrocellulose membrane. The membrane was incubated with monoclonal anti-human NR1 antibody (Invitrogen) as the primary antibody at 1:2000 dilution, followed by goat anti-mouse secondary antibody at 1:5000 dilution. NMDA NR1 was detected using an enhanced chemiluminescence detection kit (Pierce) and quantified using MultiGauge software (Fujifilm, Valhalla, NY). For calcium uptake studies, mitochondria were prepared from 10⁶ cells in locking buffer and incubated for 30 min with calcium in the absence or presence of NMDA as described above.

Statistical Analysis—Due to the lack of variation within replicates, experiments were typically carried out three times except where noted. The comparison of multiple treatment groups with controls was conducted using one-way analysis of variance with Fisher's least significant difference post-hoc testing when required. *F*-distribution calculations were performed and confirmed that, even with the small sample sizes, there was homogeneity of variance between groups. All data and error bars are presented as ±S.E.

RESULTS

Assessment of Mitochondrial Preparation Purity—We performed electron microscopy on thin sections prepared from a final mitochondrial pellet and observed an abundance of intact mitochondria and some membrane fragments but an absence of synaptosomes and other identifiable intracellular organelles (Fig. 1A). Western blot analysis confirmed the absence of cytoplasmic (β-actin), endosomal (LAMP1), endoplasmic reticulum (calnexin), and plasma (ATPase) and synaptosomal (synaptophysin) membrane contaminants (Fig. 1, B and C) in the mitochondrial (cytochrome oxidase IV) fraction. To quantify the purity of our preparation, we generated a low power electron microscopic photomontage and counted a total 1606 mitochondria yet only 51 non-mitochondrial elements. This technique therefore indicated our preparation consisted of ~97% mitochondria.

Calcium Uptake Assays—In our initial studies, mitochondria were exposed to Ca²⁺ in the presence of various compounds, and [Ca²⁺]_m was quantified in locking buffer (Fig. 2). Following exposure to the biologically active L-glutamate isoform, there was an almost 2-fold increase in [Ca²⁺]_m compared with untreated mitochondria (54.1 ± 2.3 versus 28.8 ± 2.2 fluorescence units (FU)), whereas mitochondria incubated in the presence of the same concentration of the inactive D-enantiomer showed no increase in [Ca²⁺]_m (30.4 ± 1.9 FU) (Fig. 2A). To rule out the possibility that a metabolic intermediate of glutamate was responsible for the mobilization of Ca²⁺, we exposed mitochondria to the specific synthetic agonist NMDA and observed an elevation of [Ca²⁺]_m similar in magnitude to that induced by L-glutamate (54.4 ± 2.6 FU). The highly specific

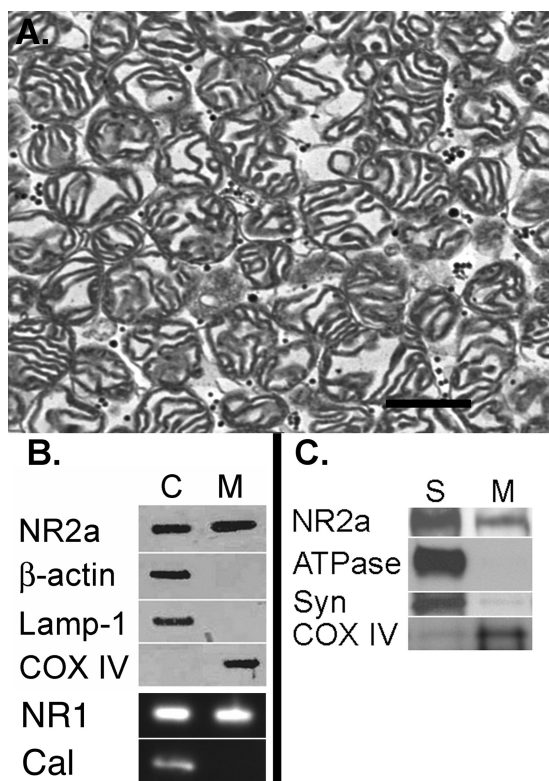


FIGURE 1. Assessment of mitochondrial purity. A, electron photomicrograph of a mitochondrial pellet reveals a sample rich in mitochondria and lacking other recognizable intracellular organelles. Scale bar = 500 nm. B, Western blot revealing both NR1 and NR2a labeling in cytosolic (C) and mitochondrial (M) samples. There was no labeling of the cytoplasmic marker β -actin, the endosomal marker LAMP1, or the endoplasmic reticulum marker calnexin (Cal) in the cytochrome oxidase IV (COX IV)-labeled mitochondrial fraction. C, there was considerably more NR2a labeling in the synaptic membrane fraction (S) compared with the mitochondrial fraction. The marker for plasma membrane (ATPase) was virtually absent in the mitochondrial fraction, and the marker for synaptic vesicles (Syn) was only minimally present.

endogenous NMDA receptor agonist quinolinic acid also caused an equivalent increase in $[Ca^{2+}]_m$ (59.6 ± 1.9 FU). The addition of the noncompetitive NMDA antagonist MK-801 ((+)-5-methyl-10,11-dihydro-5H-dibenzo[a,d]cyclohepten-5,10-imine maleate) prevented the increases in $[Ca^{2+}]_m$ induced by each of the NMDA receptor agonists (Fig. 2B). Although glycine (Fig. 2C), which is a requisite coactivator of plasma membrane NMDA receptors (27), failed to augment the effect of L-glutamate on brain mitochondria (52.3 ± 3.1 versus 54.4 ± 1.5 FU), the competitive glycine antagonist 7-chlorokynurenic acid abolished the stimulatory effect of L-glutamate (29.3 ± 3.0 versus 54.4 ± 1.5 FU).

In cells, glutamate is transported into mitochondria by carrier proteins with either the coincidental cotransport of protons into the mitochondrial matrix or in exchange for hydroxyl radicals (28). Recently, two distinct human isoforms of the transporter have been expressed in *Escherichia coli* (29). Although mitochondrial calcium uptake has not been linked to the transport of glutamate, we sought to exclude this process as a potential route of Ca^{2+} uptake. Exposure of rat brain mitochondria to L-glutamate, NMDA, or quinolinic acid in the presence of each of several glutamate transporter inhibitors failed to attenuate the glutamate-stimulated increase in $[Ca^{2+}]_m$ (Fig. 2D).

Although the use of blocking agents allowed us to uncover an NMDA-sensitive site, we wanted to determine whether NMDA could enhance mitochondrial Ca^{2+} uptake in real-time in the absence of such agents. As shown in the representative tracing (Fig. 3A), exposure of mitochondria to $5 \mu M$ Ca^{2+} resulted in a transient deflection of the fluorescent signal upward, indicating an increase in extramitochondrial Ca^{2+} , followed by a partial return to the base line, resulting from sequestration of Ca^{2+} by mitochondria. This pattern recurred three more times, after which the buffering of Ca^{2+} reached a plateau. In contrast, when mitochondria were exposed to Ca^{2+} in the presence of $10 \mu M$ NMDA, they were able to take up calcium for a total of 12 bolus additions before reaching their maximum buffering capacity (Fig. 3B). Moreover, samples co-incubated with calcium and NMDA sequestered nearly all of the calcium added to the sample.

Consistent with our findings using Calcium Green-5N, there was an $\sim 33\%$ increase in $[Ca^{2+}]_m$ using Rhod-2 following exposure to calcium and NMDA compared with untreated control mitochondria (35.78 ± 1.2 versus 26.9 ± 0.9 FU; $p < 0.001$). As predicted, D-glutamate had no effect on $[Ca^{2+}]_m$ compared with the control (27.9 ± 0.3 versus 26.9 ± 0.9 FU). Although the magnitude of change with Rhod-2 was less than that seen with Calcium Green-5N, this is likely due to the fact that Rhod-2 measures free matrix calcium and our method using Calcium Green-5N reflects total matrix calcium. The findings obtained with Rhod-2 therefore support the validity of our data using Calcium Green-5N.

Electron Microscopic Examination of NMDA Receptor Subunit NR2a—When thin sections prepared from a fixed synaptosome-derived mitochondrial pellet were labeled with an antibody against the C-terminal region of the NR2a subunit, gold particles were detected on the surface of mitochondria (Fig. 4A). Using tissue sections prepared from CA1 of the rat hippocampal formation, a region rich in plasma membrane NMDA receptors (30, 31), labeling of mitochondria was observed that was clearly above background levels (Fig. 4B) and considerably more extensive than described in two previous electromicrographic studies in which only sporadic labeling of mitochondria was noted (32, 33). Of significance, gold particles tended to occur in clusters, which are taken as an index of specific epitope recognition. No gold particles were associated with mitochondria when the primary antibody was omitted in either preparation.

Submitochondrial Localization of NR1 and NR2a—To elucidate which mitochondrial membrane(s) NMDA receptor units were located, the OMM was solubilized and stripped from the inner membrane, and both fractions were probed with antibodies against NR1 and NR2a. As shown Fig. 4C, both NR1 and NR2a immunoreactivities were noted only in the inner membrane fraction.

Effect of NMDA Receptor Overexpression in Mitochondria—In light of the previous findings, we selectively overexpressed NMDA receptors on mitochondria and examined the effects in an *in vitro* model of excitotoxicity. To accomplish this, we targeted NR1 and NR2a subunits, the coexpression of which results in a functional receptor with pharmacological characteristics nearly indistinguishable from the of native NMDA

NMDA Enhances Calcium Uptake in Isolated Mitochondria

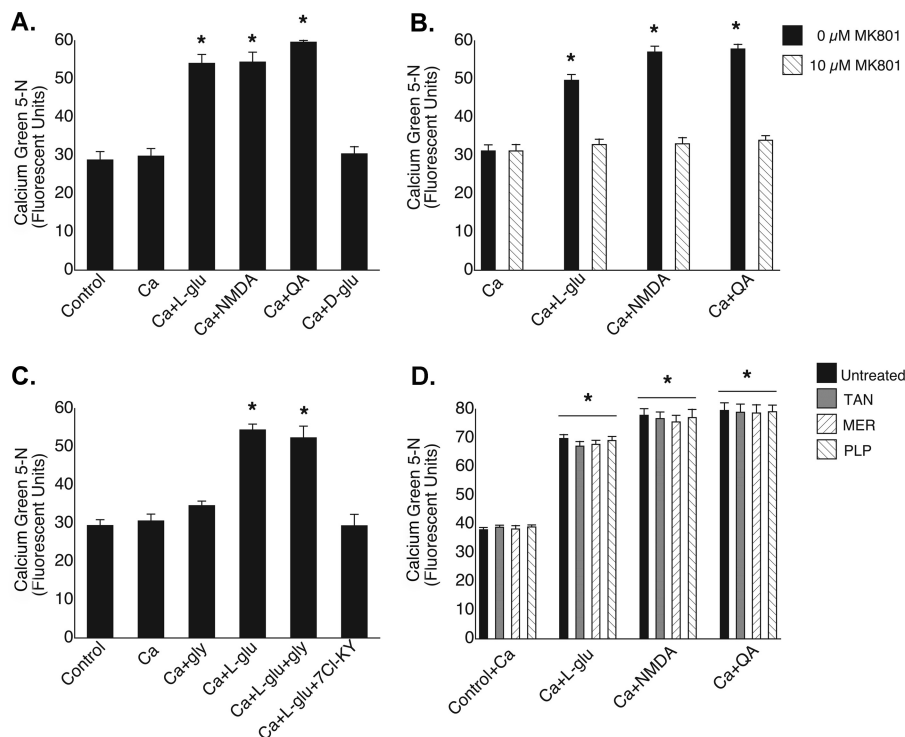


FIGURE 2. Pharmacological profile of mitochondrial NMDA-binding site. A, influx of Ca^{2+} into mitochondria was stimulated by L-glutamate ($250 \mu\text{M}$), NMDA ($10 \mu\text{M}$), and quinolinic acid (QA; $10 \mu\text{M}$). The biologically inactive D-glutamate isoform ($250 \mu\text{M}$) failed to increase $[\text{Ca}^{2+}]_m$. *, $p < 0.001$ versus the control. B, NMDA receptor agonist-induced increases in $[\text{Ca}^{2+}]_m$ were blocked by MK-801 ($10 \mu\text{M}$). *, $p < 0.001$ versus Ca^{2+} . C, L-glutamate-induced increases in $[\text{Ca}^{2+}]_m$ were not inhibited by glycine ($100 \mu\text{M}$) but were blocked by 7-chlorokynurenic acid (7Cl-KY; $10 \mu\text{M}$). *, $p < 0.001$ versus the control. D, the mitochondrial glutamate transporter inhibitors tannic acid (TAN; $25 \mu\text{M}$), mersalyl (MER; $100 \mu\text{M}$), and pyridoxal 5'-phosphate (PLP; $100 \mu\text{M}$) failed to attenuate NMDA agonist-induced increases in $[\text{Ca}^{2+}]_m$. *, $p < 0.001$ versus the respective controls.

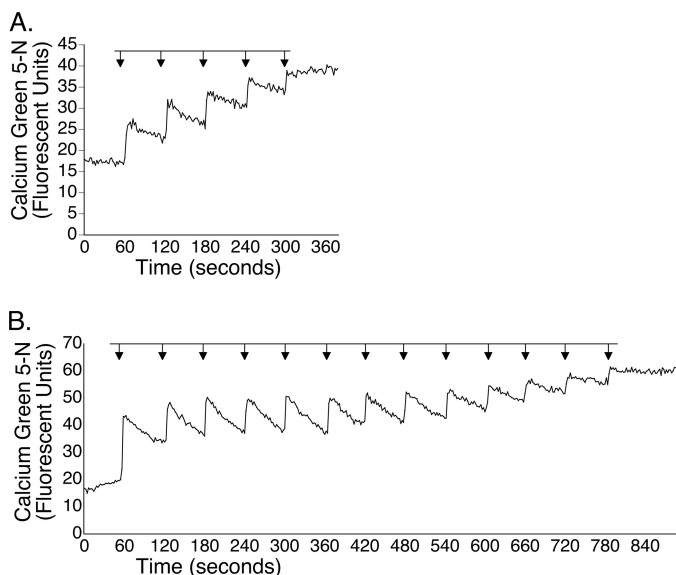


FIGURE 3. NMDA enhances mitochondrial uptake of Ca^{2+} . Mitochondria ($250 \mu\text{g}$) were exposed to $5 \mu\text{M}$ bolus additions of Ca^{2+} in the absence (A) or presence (B) of $10 \mu\text{M}$ NMDA. In the absence of NMDA, mitochondria partially buffered four bolus additions of Ca^{2+} before uptake reached a plateau. When NMDA was included, mitochondria sequestered a total of 13 bolus additions before reaching maximum buffering capacity.

receptors (34), into mitochondrial membranes of GT1-7 cells using a Bcl-2 leader sequence. This leader sequence has been shown to insert Bcl-2 into both the outer (35) and inner (36) mitochondrial membranes. GT1-7 is an immortalized gonadotropin-releasing hormone neuronal cell line (37) with well

characterized plasma membrane NMDA receptors (38). In non-transfected cells, both NR2a and NR1 proteins were found in the mitochondrial and plasma membrane fractions, respectively (Fig. 5A). In cells transfected with NR1-NR2a, there was an ~5-fold increase in both mitochondrial subunits (Fig. 5A), with no discernible change in plasma membrane levels. Twenty-four h following a brief exposure of non-transfected cells to $25 \mu\text{M}$ L-glutamate, there was ~35% cell death (Fig. 5B). In cells transfected with the NR1-NR2a cassette 48 h prior to glutamate treatment, cell death was reduced to ~10%. Transfection of GT1-7 cells with mutant NR1-NR2a conferred no neuroprotection.

In a parallel experiment, GT1-7 cells were incubated with L-glutamate, after which the mitochondria were isolated, and $[\text{Ca}^{2+}]_m$ was quantified (Fig. 5C). Transfected cells that were not exposed to glutamate revealed nearly identical levels of $[\text{Ca}^{2+}]_m$ as non-transfected control cells (39.3 ± 1.7 versus 40.2 ± 1.6 FU), indicating that the overexpression on NMDA receptors alone did not facilitate the influx of calcium into mitochondria. In contrast, the addition of L-glutamate to non-transfected cells resulted in an ~25% increase in $[\text{Ca}^{2+}]_m$ compared with untreated non-transfected cells (50.92 ± 1.0 versus 41.8 ± 1.8 FU) (Fig. 5C), whereas NR1-NR2a-transfected cells exposed to L-glutamate revealed a >2-fold increase in $[\text{Ca}^{2+}]_m$ (87.9 ± 1.8 versus 41.8 ± 1.8 FU). Cells transfected with mutant NR1-NR2a showed an increase in $[\text{Ca}^{2+}]_m$ similar in magnitude to that seen in non-transfected cells exposed to L-glutamate (53.1 ± 1.2 versus 50.92 ± 1.0 FU).

We next examined the effect of transfection with a Bcl-2-NR1-NR2a fusion protein on ATP production following an

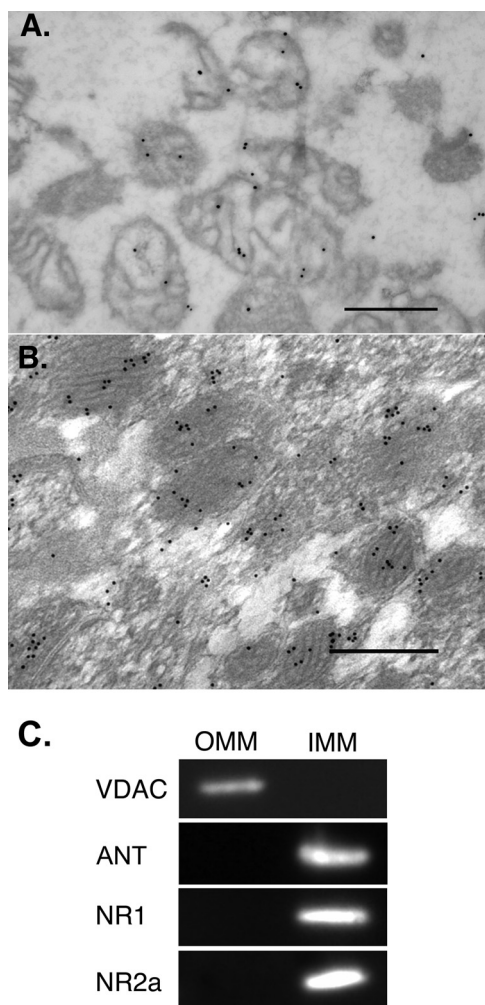


FIGURE 4. Mitochondrial localization of NMDA receptor. Post-embedding immunogold labeling of NR2a and electron microscopy revealed gold particles overlying mitochondria in a pellet (A) and *in situ* (B). Scale bars = 500 nm. C, OMM fractions were selectively labeled with an antibody directed against the voltage-dependent anion channel (VDAC), and IMM fractions were selectively labeled with an antibody against the adenine nucleotide translocator (ANT). Note that both NR1 and NR2a were confined to the IMM.

excitotoxic insult (Fig. 5D). Compared with ATP levels in untreated non-transfected cells (1.9 ± 0.03 pmol), cellular ATP levels in cells transfected with either NR1-NR2a or mutant NR1-NR2a were unchanged (1.9 ± 0.02 and 1.9 ± 0.03 pmol, respectively), indicating that transfection itself has no effect on basal cellular ATP levels. In non-transfected cells briefly exposed to $25 \mu\text{M}$ L-glutamate, there was also no increase in cellular ATP levels (2.1 ± 0.02 pmol). In contrast, when cells transfected with NR1-NR2a were treated with glutamate, there was a 2-fold increase in ATP levels (4.1 ± 0.22 pmol), whereas glutamate treatment of mutant NR1-NR2a-transfected cells resulted in basal levels of ATP (2.0 ± 0.02 pmol).

Effect of Silencing NMDA Receptor Subunit NR1 on Mitochondrial Calcium Uptake—The ability of mitochondria to sequester Ca^{2+} was examined in GT1-7 cells treated with siRNA against the NR1 subunit, the presence of which is needed for successful targeting of NR2a into the plasma membrane (39). In mitochondria isolated from cells transfected with siRNA against NR1, there was an $\sim 65\%$ reduction in mitochon-

drial NR1 protein expression (Fig. 6, A and B). Preparations of mitochondria from non-transfected (control) cells and siRNA- and scrambled RNA-transfected cells all demonstrated similar levels of $[\text{Ca}^{2+}]_m$ following a 30-min incubation in the presence of calcium (Fig. 6C). Consistent with our initial findings (Fig. 2A), when mitochondria isolated from non-transfected GT1-7 cells were exposed to both NMDA and calcium, there was an ~ 2 -fold increase compared with mitochondria exposed to calcium alone. When NR1 was silenced, however, exposure to calcium and NMDA did not increase $[\text{Ca}^{2+}]_m$. In contrast, when mitochondria were prepared from cells transfected with scrambled siRNA, the ability to sequester calcium returned to control levels, as revealed by a 2-fold increase in $[\text{Ca}^{2+}]_m$ following exposure to both calcium and NMDA compared with mitochondria in which there was no change in NR1 protein expression.

DISCUSSION

Currently, two principal routes have been described by which calcium can enter nervous system mitochondria: the high capacity mitochondrial uniporter (9) and low capacity RAM (10). The uptake of calcium via the uniporter, the structure of which has recently been described (40), is driven by the mitochondrial membrane potential and has been linked to both energy production (41, 42) and cell death pathways via induction of the mitochondrial permeability transition (43). The role of RAM is less clear. The results of this study indicate that there may yet be another conduit for calcium entry that is activated by traditional NMDA receptor agonists. To unmask this effect, both the calcium uniporter and RAM, as well as efflux pathways, were blocked during our initial studies to prevent movement of calcium via these pathways. The lack of increase in $[\text{Ca}^{2+}]_m$ in “locked” mitochondria exposed to calcium compared with control mitochondria (Fig. 1A) strongly suggests that the accumulation of calcium following treatment with NMDA agonists cannot be ascribed to the uptake of calcium through these known channels. Moreover, our findings indicate that glutamate transporters are not responsible for the entrance of calcium into mitochondria. Real-time calcium measurements in “unlocked” mitochondria confirmed these observations and further suggest that glutamate-like compounds enhance mitochondrial calcium retention capacity.

Several steps were taken to ensure the purity of the mitochondrial preparations. First, samples were subjected to rapid decompression in a nitrogen cell bomb, which ruptures synaptosomes, thereby eliminating them from the preparation (24). The resultant samples, which were then centrifuged through a Percoll gradient and washed several times to remove other contaminants, were shown to be free of synaptosomes and other potential membrane compartments based on electron microscopic and Western blot analyses. In light of the high degree of purity ($\sim 97\%$) of the preparations, we conclude that the elevation in $[\text{Ca}^{2+}]_m$ following exposure to NMDA agonists is the result of accumulation of this ion in mitochondria and not other compartments.

In this study, uptake of Ca^{2+} by non-transfected and mutant NR1-NR2a-transfected cells following treatment with glutamate showed an $\sim 25\%$ increase in $[\text{Ca}^{2+}]_m$, which was associ-

NMDA Enhances Calcium Uptake in Isolated Mitochondria

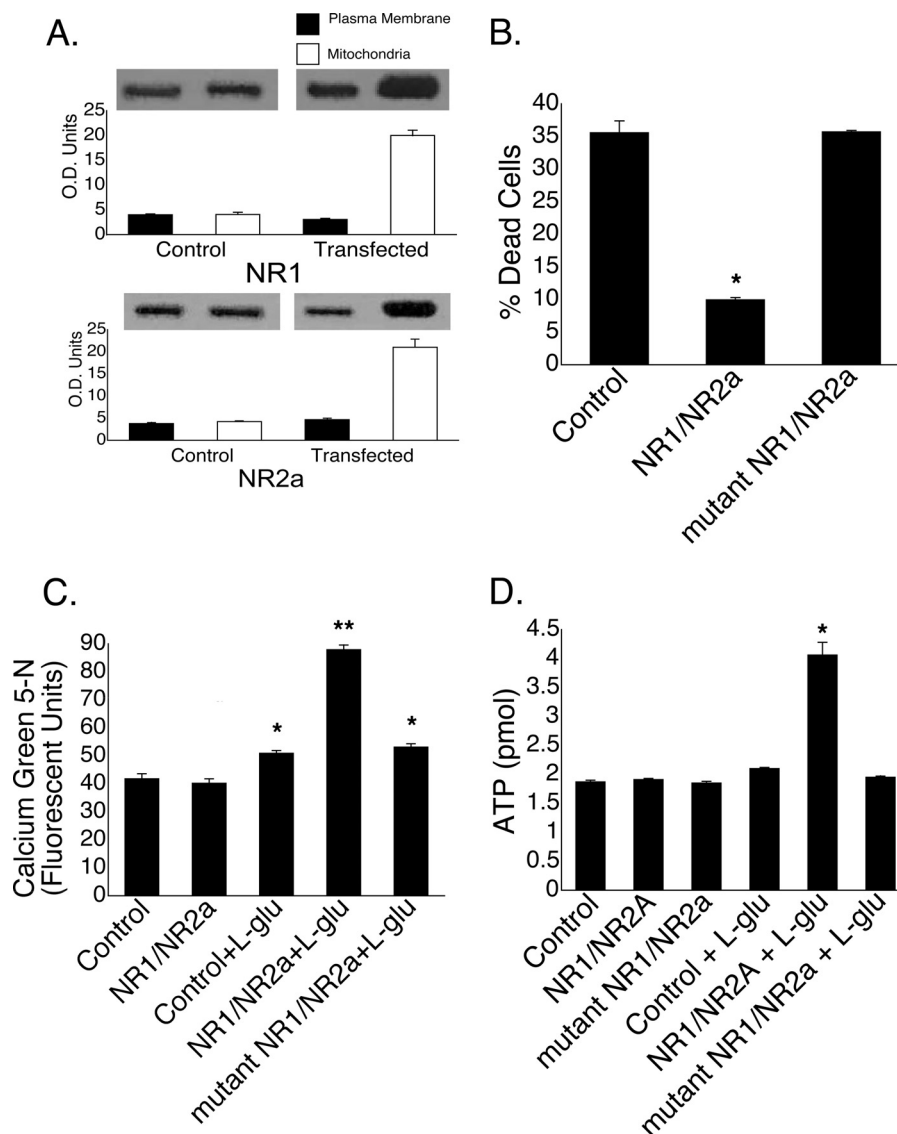


FIGURE 5. Transfection of GT1-7 neurons with NR1-NR2a is neuroprotective. *A*, compared with non-transfected control cells, transfection resulted in a selective increase in both NR1 and NR2a protein expression in mitochondria demonstrated by Western blotting (quantified in optical density units). *B*, cell death was reduced by ~60% in transfected GT1-7 cells 24 h following exposure to L-glutamate compared with either non-transfected cells or cells transfected with mutant NR1-NR2a. *C*, both control cells and NR1-NR2a-transfected cells had equivalent levels of mitochondrial calcium following a 30-min incubation in the absence of L-glutamate. A slight but significant elevation in $[Ca^{2+}]_m$ was seen in both non-transfected control cells and cells transfected with mutant NR1-NR2a following a 30-min exposure to L-glutamate compared with untreated control cells. In contrast, exposure of NR1-NR2a-transfected cells to L-glutamate caused a 2-fold increase in $[Ca^{2+}]_m$ compared with untreated non-transfected control cells. *, $p < 0.01$ versus the control; **, $p < 0.001$ versus the control + L-glutamate. *D*, ATP levels doubled in GT1-7 cells transfected with NR1-NR2a but not mutant NR1-NR2a after exposure to L-glutamate. *, $p < 0.001$ versus the control.

ated with ~35% cell death. In contrast, in cells overexpressing NR1-NR2a, treatment with glutamate caused a 2-fold increase in $[Ca^{2+}]_m$, yet cell death was significantly depressed. These findings suggest that Ca^{2+} taken up via NMDA receptors targeting mitochondria may serve a very different role. Because increases in $[Ca^{2+}]_m$ can activate several enzymes of the TCA cycle with the subsequent production of NADH (44, 45), we speculate that activation of mitochondrial NMDA-sensitive sites provides an early signal to stimulate oxidative phosphorylation in an attempt to enhance energy supplies and mitigate damage that might otherwise proceed unchecked in an excitotoxic environment. The coincidental increase of ATP production in NR1-NR2a-transfected cells following exposure of cells to glutamate supports this notion.

One issue that was not addressed in this study is the mechanism whereby the mitochondrial NMDA-sensitive site can initiate a specific response in the presence of millimolar levels of cytoplasmic glutamate. Two possible explanations can be offered. First, it has been demonstrated that following the stimulation of plasma membrane NMDA receptors, there is an increase in cytosolic calcium and that this pool of calcium has privileged access to mitochondria (11). On the basis of our findings, we would posit that due to the high levels of glutamate, this site is constitutively active, but only following an increase in cytosolic calcium "microdomains" resulting from plasma membrane NMDA receptor activation can calcium specifically enter the mitochondria. Indeed, calcium microdomains have been shown to regulate a number of cellular processes in distinct

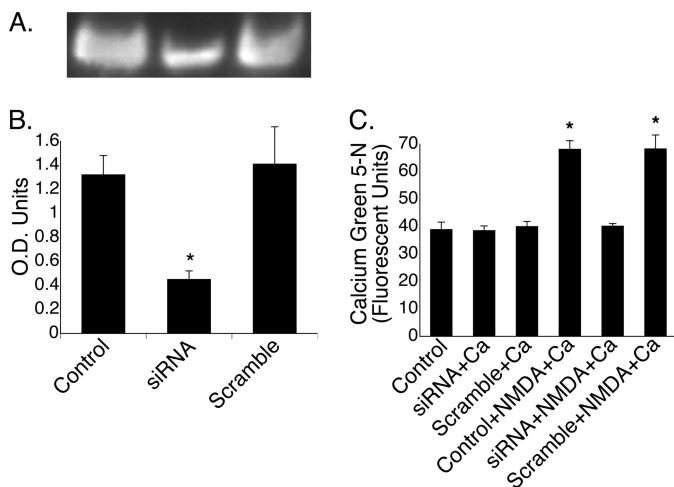


FIGURE 6. Anti-NR1 siRNA attenuates mitochondrial uptake of Ca^{2+} . GT1-7 cells were transfected with siRNA against NR1 for 72 h, which resulted in reduced NR1 protein expression (A), which is quantified in optical density units (B). *, $p < 0.001$. C, mitochondria isolated from cells transfected with siRNA or scrambled RNA that were exposed to calcium had base-line (control) $[\text{Ca}^{2+}]_m$ levels. As demonstrated in Fig. 2, mitochondria prepared from control cells and exposed to both calcium and NMDA showed a 2-fold increase in $[\text{Ca}^{2+}]_m$. In contrast, cells in which NR1 was knocked down failed to take up Ca^{2+} following the addition of NMDA and calcium, whereas scrambled RNA-transfected cells, like control cells, showed an ~2-fold increase in $[\text{Ca}^{2+}]_m$ under similar conditions. *, $p < 0.001$ versus the control.

regions of the cell (46). Second, it is conceivable that there is another messenger that, in the presence of elevated calcium, activates the mitochondrial NMDA-sensitive site. The location of both NR1 and NR2a subunits in the inner mitochondrial membrane is consistent with the role of this site as a point of calcium entry into the matrix, yet how they target this structure requires investigation.

The elevation in $[\text{Ca}^{2+}]_m$ following treatment with known receptor agonists and antagonists suggests that there exists a site with characteristics similar to plasma membrane NMDA receptors. The observed immunoreactivity against NR2a and the prevention of calcium uptake in mitochondria in which NR1 was silenced further suggest that this site shares sequence homology with plasma membrane NMDA receptors. It is not clear, however, whether this site is distinct or part of a larger molecular entity. The ability of mitochondria to sequester calcium in the presence of inhibitors of both the calcium uniporter and permeability transition argues against an association with either of these structures. Studies are currently underway to identify and further characterize the nature of this putative receptor.

Acknowledgments—We are grateful to Dr. Paul Whiting (Merck Sharp and Dohme) for providing human NR1 and NR2a cDNA constructs and Dr. Pamela Mellon (Salk Institute for Biological Studies) for providing GT1-7 cells. We appreciate the constructive comments of and discussions with Drs. Franca Cambi, John W. Olney, Daret K. St. Clair, John T. Slevin, and Patrick G. Sullivan. The expert assistance of Dr. Bruce Maley and Mary Gail Engle (University of Kentucky Electron Microscopy and Imaging Facility) and Sarah Kennedy and Jesse Dean with electron microscopic studies is greatly appreciated. The assistance of Drs. Edward Lesnefsky and Qun Chen with real-time calcium measurements is greatly appreciated.

REFERENCES

- Bliss, T. V., and Collingridge, G. L. (1993) A synaptic model of memory: long-term potentiation in the hippocampus. *Nature* **361**, 31–39
- Kaul, M., Garden, G. A., and Lipton, S. A. (2001) Pathways to neuronal injury and apoptosis in HIV-associated dementia. *Nature* **410**, 988–994
- Lancelot, E., and Beal, M. F. (1998) Glutamate toxicity in chronic neurodegenerative disease. *Prog. Brain Res.* **116**, 331–347
- Zipfel, G. J., Babcock, D. J., Lee, J. M., and Choi, D. W. (2000) Neuronal apoptosis after CNS injury: the roles of glutamate and calcium. *J. Neurotrauma* **17**, 857–869
- Hardingham, G. E. (2009) Coupling of the NMDA receptor to neuroprotective and neurodestructive events. *Biochem. Soc. Trans.* **37**, 1147–1160
- Budd, S. L., and Nicholls, D. G. (1996) Mitochondria, calcium regulation, and acute glutamate excitotoxicity in cultured cerebellar granule cells. *J. Neurochem.* **67**, 2282–2291
- Khodorov, B., Pinelis, V., Storozhevych, T., Vergun, O., and Vinskaya, N. (1996) Dominant role of mitochondria in protection against a delayed neuronal Ca^{2+} overload induced by endogenous excitatory amino acids following a glutamate pulse. *FEBS Lett.* **393**, 135–138
- White, R. J., and Reynolds, I. J. (1996) Mitochondrial depolarization in glutamate-stimulated neurons: an early signal specific to excitotoxin exposure. *J. Neurosci.* **16**, 5688–5697
- Gunter, T. E., Buntinas, L., Sparagna, G. C., and Gunter, K. K. (1998) The Ca^{2+} transport mechanisms of mitochondria and Ca^{2+} uptake from physiological-type Ca^{2+} transients. *Biochim. Biophys. Acta* **1366**, 5–15
- Buntinas, L., Gunter, K. K., Sparagna, G. C., and Gunter, T. E. (2001) The rapid mode of calcium uptake into heart mitochondria (RaM): comparison to RaM in liver mitochondria. *Biochim. Biophys. Acta* **1504**, 248–261
- Peng, T. L., and Greenamyre, J. T. (1998) Privileged access to mitochondria of calcium influx through N-methyl-D-aspartate receptors. *Mol. Pharmacol.* **53**, 974–980
- Chenu, C., Serre, C. M., Raynal, C., Burt-Pichat, B., and Delmas, P. D. (1998) Glutamate receptors are expressed by bone cells and are involved in bone resorption. *Bone* **22**, 295–299
- Franconi, F., Miceli, M., Alberti, L., Seghieri, G., De Montis, M. G., and Tagliamonte, A. (1998) Further insights into the anti-aggregating activity of NMDA in human platelets. *Br. J. Pharmacol.* **124**, 35–40
- Genever, P. G., Maxfield, S. J., Kennovin, G. D., Maltman, J., Bowgen, C. J., Raxworthy, M. J., and Skerry, T. M. (1999) Evidence for a novel glutamate-mediated signaling pathway in keratinocytes. *J. Invest. Dermatol.* **112**, 337–342
- Morhenn, V. B., Waleh, N. S., Mansbridge, J. N., Unson, D., Zolotarev, A., Cline, P., and Toll, L. (1994) Evidence for an NMDA receptor subunit in human keratinocytes and rat cardiocytes. *Eur. J. Pharmacol.* **268**, 409–414
- Rzeski, W., Turski, L., and Ikonomidou, C. (2001) Glutamate antagonists limit tumor growth. *Proc. Natl. Acad. Sci. U.S.A.* **98**, 6372–6377
- Takano, T., Lin, J. H., Arcuino, G., Gao, Q., Yang, J., and Nedergaard, M. (2001) Glutamate release promotes growth of malignant gliomas. *Nat. Med.* **7**, 1010–1015
- Patton, A. J., Genever, P. G., Birch, M. A., Suva, L. J., and Skerry, T. M. (1998) Expression of an N-methyl-D-aspartate-type receptor by human and rat osteoblasts and osteoclasts suggests a novel glutamate signaling pathway in bone. *Bone* **22**, 645–649
- Genever, P. G., Wilkinson, D. J., Patton, A. J., Peet, N. M., Hong, Y., Mathur, A., Erusalimsky, J. D., and Skerry, T. M. (1999) Expression of a functional N-methyl-D-aspartate-type glutamate receptor by bone marrow megakaryocytes. *Blood* **93**, 2876–2883
- Purcell, W. M., Doyle, K. M., Westgate, C., and Atterwill, C. K. (1996) Characterization of a functional polyamine site on rat mast cells: association with an NMDA receptor macrocomplex. *J. Neuroimmunol.* **65**, 49–53
- Skerry, T. M., and Genever, P. G. (2001) Glutamate signaling in non-neuronal tissues. *Trends Pharmacol. Sci.* **22**, 174–181
- Maechler, P., and Wollheim, C. B. (1999) Mitochondrial glutamate acts as a messenger in glucose-induced insulin exocytosis. *Nature* **402**, 685–689
- MacDonald, M. J., and Fahien, L. A. (2000) Glutamate is not a messenger

NMDA Enhances Calcium Uptake in Isolated Mitochondria

- in insulin secretion. *J. Biol. Chem.* **275**, 34025–34027
24. Brown, M. R., Sullivan, P. G., Dorenbos, K. A., Modafferi, E. A., Geddes, J. W., and Steward, O. (2004) Nitrogen disruption of synaptoneurosomes: an alternative method to isolate brain mitochondria. *J. Neurosci. Methods* **137**, 299–303
 25. Korde, A. S., Pettigrew, L. C., Craddock, S. D., Pocernich, C. B., Waldmeier, P. C., and Maragos, W. F. (2007) Protective effects of NIM811 in transient focal cerebral ischemia suggest involvement of the mitochondrial permeability transition. *J. Neurotrauma* **24**, 895–908
 26. Korde, A. S., Sullivan, P. G., and Maragos, W. F. (2005) The uncoupling agent 2,4-dinitrophenol improves mitochondrial homeostasis following striatal quinolinic acid injections. *J. Neurotrauma* **22**, 1142–1149
 27. Kleckner, N. W., and Dingledine, R. (1988) Requirement for glycine in activation of NMDA receptors expressed in *Xenopus* oocytes. *Science* **241**, 835–837
 28. Kraemer, R., and Palmieri, F. (1992) *Molecular Mechanisms in Bioenergetics*, pp. 359–384, Elsevier Science Publishers B.V., Amsterdam
 29. Fiermonte, G., Palmieri, L., Todisco, S., Agrimi, G., Palmieri, F., and Walker, J. E. (2002) Identification of the mitochondrial glutamate transporter. Bacterial expression, reconstitution, functional characterization, and tissue distribution of two human isoforms. *J. Biol. Chem.* **277**, 19289–19294
 30. Greenamyre, J. T., Olson, J. M., Penney, J. B., Jr., and Young, A. B. (1985) Autoradiographic characterization of *N*-methyl-D-aspartate-, quisqualate-, and kainate-sensitive glutamate-binding sites. *J. Pharmacol. Exp. Ther.* **233**, 254–263
 31. Maragos, W. F., Penney, J. B., and Young, A. B. (1988) Anatomic correlation of NMDA and [³H]TCP-labeled receptors in rat brain. *J. Neurosci.* **8**, 493–501
 32. Huntley, G. W., Vickers, J. C., Janssen, W., Brose, N., Heinemann, S. F., and Morrison, J. H. (1994) Distribution and synaptic localization of immunocytochemically identified NMDA receptor subunit proteins in sensory motor and visual cortices of monkey and human. *J. Neurosci.* **14**, 3603–3619
 33. Petralia, R. S., Yokotani, N., and Wenthold, R. J. (1994) Light and electron microscope distribution of the NMDA receptor subunit NMDAR1 in the rat nervous system using a selective anti-peptide antibody. *J. Neurosci.* **14**, 667–696
 34. Le Bourdellès, B., Wafford, K. A., Kemp, J. A., Marshall, G., Bain, C., Wilcox, A. S., Sikela, J. M., and Whiting, P. J. (1994) Cloning, functional coexpression, and pharmacological characterization of human cDNAs encoding NMDA receptor NR1 and NR2a subunits. *J. Neurochem.* **62**, 2091–2098
 35. Nguyen, M., Millar, D. G., Yong, V. W., Korsmeyer, S. J., and Shore, G. C. (1993) Targeting of Bcl-2 to the mitochondrial outer membrane by a COOH-terminal signal anchor sequence. *J. Biol. Chem.* **268**, 25265–25268
 36. Hockenbery, D., Nuñez, G., Millman, C., Schreiber, R. D., and Korsmeyer, S. J. (1990) Bcl-2 is an inner mitochondrial membrane protein that blocks programmed cell death. *Nature* **348**, 334–336
 37. Mellon, P. L., Windle, J. J., Goldsmith, P. C., Padula, C. A., Roberts, J. L., and Weiner, R. I. (1990) Immortalization of hypothalamic GnRH neurons by genetically targeted tumorigenesis. *Neuron* **5**, 1–10
 38. Mahesh, V. B., Zamorano, P., De Sevilla, L., Lewis, D., and Brann, D. W. (1999) Characterization of ionotropic glutamate receptors in rat hypothalamus, pituitary, and immortalized gonadotropin-releasing hormone (GnRH) neurons (GT1-7 cells). *Neuroendocrinology* **69**, 397–407
 39. McIlhinney, R. A., Le Bourdellès, B., Molnár, E., Tricaud, N., Streit, P., and Whiting, P. J. (1998) Assembly, intracellular targeting, and cell surface expression of the human *N*-methyl-D-aspartate receptor subunits NR1a and NR2a in transfected cells. *Neuropharmacology* **37**, 1355–1367
 40. De Stefani, D., Raffaello, A., Teardo, E., Szabò, I., and Rizzuto, R. (2011) A forty-kilodalton protein of the inner membrane is the mitochondrial calcium uniporter. *Nature* **476**, 336–340
 41. Robb-Gaspers, L. D., Burnett, P., Rutter, G. A., Denton, R. M., Rizzuto, R., and Thomas, A. P. (1998) Integrating cytosolic calcium signals into mitochondrial metabolic responses. *EMBO J.* **17**, 4987–5000
 42. Celsi, F., Pizzo, P., Brini, M., Leo, S., Fotino, C., Pinton, P., and Rizzuto, R. (2009) Mitochondria, calcium, and cell death: a deadly triad in neurodegeneration. *Biochim. Biophys. Acta* **1787**, 335–344
 43. Ricchelli, F., Sileikyte, J., and Bernardi, P. (2011) Shedding light on the mitochondrial permeability transition. *Biochim. Biophys. Acta* **1807**, 482–490
 44. Denton, R. M., Rutter, G. A., Midgley, P. J., and McCormack, J. G. (1988) Effects of Ca²⁺ on the activities of the calcium-sensitive dehydrogenases within the mitochondria of mammalian tissues. *J. Cardiovasc. Pharmacol.* **12**, 69–72
 45. Hansford, R. G. (1994) Physiological role of mitochondrial Ca²⁺ transport. *J. Bioenerg. Biomembr.* **26**, 495–508
 46. Berridge, M. J. (2006) Calcium microdomains: organization and function. *Cell Calcium* **40**, 405–412